Since January 2020 Elsevier has created a COVID-19 resource centre with free information in English and Mandarin on the novel coronavirus COVID-19. The COVID-19 resource centre is hosted on Elsevier Connect, the company's public news and information website.

BASIC SCIENCE

Nanomedicine: Nanotechnology, Biology, and Medicine
40 (2022) 102498

nanomedicine
Nanotechnology, Biology, and Medicine

Original Article

nanomedjournal.com

Lung function improves after delayed treatment with CNP-miR146a following acute lung injury

Stephen M. Niemiec, MD[a], Sarah A. Hilton, MD[a], Alison Wallbank, BS[b], Amanda E. Louiselle, MD[a], Hanan Elajaili, PhD[c], Junyi Hu, MD[a], Sushant Singh, PhD[d,e], Sudipta Seal, PhD[e,f], Eva Nozik, MD[c], Bradford Smith, PhD[b], Carlos Zgheib, PhD[a], Kenneth W. Liechty, MD[a,*]

[a]*Laboratory for Fetal and Regenerative Biology, Department of Surgery, University of Colorado Denver School of Medicine and Children's Hospital Colorado, Aurora, CO, USA*

[b]*Department of Bioengineering, University of Colorado Denver | Anschutz Medical Campus, Aurora, CO, USA*

[c]*Cardiovascular Pulmonary Research Laboratories and Pediatric Critical Care Medicine, Department of Pediatrics, University of Colorado, Aurora, CO, USA*

[d]*Amity Institute of Biotechnology, Amity University Chhattisgarh, Raipur, Chhattisgarh, India*

[e]*Department of Material Science and Engineering, Advanced Materials Processing and Analysis Center, Nanoscience Technology Center, University of Central Florida, Orlando, FL, USA*

[f]*College of Medicine, UCF Prosthetics Cluster, University of Central Florida, Orlando, FL, USA*

Revised 9 October 2021

Abstract

Acute respiratory distress syndrome (ARDS) is a highly morbid pulmonary disease characterized by hypoxic respiratory failure. Its pathogenesis is characterized by unrestrained oxidative stress and inflammation, with long-term sequelae of pulmonary fibrosis and diminished lung function. Unfortunately, prior therapeutic ARDS trials have failed and therapy is limited to supportive measures. Free radical scavenging cerium oxide nanoparticles (CNP) conjugated to the anti-inflammatory microRNA-146a (miR146a), termed CNP-miR146a, have been shown to prevent acute lung injury in a pre-clinical model. In this study, we evaluated the potential of delayed treatment with CNP-miR146a at three or seven days after injury to rescue the lung from acute injury. We found that intratracheal CNP-miR146a administered three days after injury lowers pulmonary leukocyte infiltration, reduce inflammation and oxidative stress, lower pro-fibrotic gene expression and collagen deposition in the lung, and ultimately improve pulmonary function.

Key words: Acute respiratory distress syndrome; Cerium oxide nanoparticles (CNP); microRNA-146a (miR146a); Acute lung injury; Pulmonary fibrosis

The ongoing novel coronavirus (SARS-CoV-2) pandemic has highlighted the need for therapeutic innovation in the treatment of acute lung injury (ALI) and acute respiratory distress syndrome (ARDS), a severe pulmonary disease characterized by hypoxic respiratory failure affecting nearly 200,000 individuals annually in the United States alone.[1] Worldwide, ARDS accounts for over 10% of all intensive care unit (ICU) admissions with the incidence increasing in the past year secondary to the global pandemic.[1–4] Mortality with moderate to severe ARDS is nearly 40%, and patients who survive their initial hospitalization are at increased risk of long-term pulmonary disease secondary to fibrotic changes in the lung.[5,6] Unfortunately, therapies are largely limited to supportive strategies such as mechanical ventilation and prone positioning.[3,7]

ARDS can be triggered by a range of etiologies, such as pneumonia or trauma, but all share the common pathways of an unrestrained inflammatory response and profound oxidative stress. These inflammatory pathways have been shown to be key

Conflicts of interest and source of funding: This work was supported by a Gates Center Grubstake Award for the work presented in this publication. Additionally, S.Seal, E.N., C.Z., and K.L. report financial interest in Ceria Therapeutics.

* Corresponding author at: Barbara Davis Center for Childhood Diabetes, Aurora, CO.
E-mail address: ken.liechty@cuanschutz.edu (K.W. Liechty).

https://doi.org/10.1016/j.nano.2021.102498
1549-9634/

Please cite this article as: Niemiec SM, et al, Lung function improves after delayed treatment with CNP-miR146a following acute lung injury. *Nanomedicine: NBM* 2022;40:102498, https://doi.org/10.1016/j.nano.2021.102498

mediators in the pathogenesis of ALI and ARDS.[8–10] Studies have shown that higher levels of interleukin (IL)-6 and tissue necrosis factor (TNF) α in patients with ARDS are associated with increased morbidity and mortality.[11,12] The inflammatory response results in pulmonary edema and worsening hypoxia, and promotes downstream fibrotic changes in the lung.[13] Therefore, therapeutics that inhibit the inflammatory cascade could offer a promising avenue for the treatment of ALI/ARDS.

One class of small molecules being studied for the treatment of acute lung injury is the microRNAs (miRNA, miR).[14] One such miRNA, miR146a, is an anti-inflammatory miRNA that inhibits the nuclear factor kappa B (NFκB) pathway through upstream inhibition of tumor necrosis factor receptor associate factor (TRAF) 6 and IL-1 receptor associated kinase (IRAK) 1.[15,16] NFκB activation normally upregulates pro-inflammatory IL-6, IL-8, and TNFα, so inhibition of the NFκB pathway with miR146a is able to lower pro-inflammatory signaling in lung disease.[17,18] Because miRNAs are quickly degraded, nanoparticle technology is often used to improve miRNA stability and improve therapeutic delivery to the target organ. miR146a delivery with liposomal nanoparticles has been shown to decrease ventilator-induced lung injury.[19] Cerium oxide nanoparticles (CNP) are a divalent metal oxide that can conjugate to and stabilize miRNAs for therapeutic use.[20] Unlike some other nanoparticle delivery systems, the divalent nature of CNP offers the synergistic therapeutic benefit of lowering reactive oxygen species levels by acting as a free radical scavenger.[8,21–26] CNP have had recent implications as a potential treatment for coronavirus-associated ARDS.[27] Furthermore, CNP have been shown to inhibit transforming growth factor (TGF)-β, which is an important mediator of ARDS-associated pulmonary fibrosis.[28,29]

Previous research has shown that a single intratracheal (IT) dose of CNP-miR146a is able to prevent ALI in a murine bleomycin injury model.[20] The IT drug delivery route allows for localized therapeutic delivery to the lung while minimizing systemic absorption and avoiding first-pass drug degradation common with intravenous and gastrointestinal administration.[20,30] Treatment at the time of injury provides a mechanistic understanding of ALI pathophysiology and the role of CNP-miR146a in decreasing the injury cascade. Preventative treatment could be applied to patients who have an observed aspiration event or are placed on the ventilator for surgery; however, the majority of patients with ALI will present hours to days after onset of injury, after which the inflammatory cascade has already been initiated and lung function has deteriorated. Therefore, it is critical to examine the efficacy of delayed treatment with novel therapeutics like CNP-miR146a after the onset of oxidative stress and inflammatory signaling. We hypothesized that delayed treatment with CNP-miR146a three or seven days following acute injury with bleomycin would rescue pulmonary function by decreasing oxidative stress, inflammation, and fibrosis in the lung.

Methods

Development of cerium oxide nanoparticles and miR146a conjugation

The synthesis of CNP, also named nanoceria, has previously been described in detail.[31,32] Briefly, $Ce(NO)_3$, $6H_2O$ was mixed and dissolved in deionized water. Excess hydrogen peroxide was then added to oxidize the cerium (III) ions to cerium (IV) oxide at a pH below 3.5. The acidic pH maintains nanoparticle suspension. Oxidized nanoparticles precipitate into crystalline structures, which are then isolated with centrifugation. Nanoceria is resuspended in RNase-free water to a final concentration of 10 μM. To conjugate miR146a to CNP, 1,1-carbonyldiimidazole (CDI) is activated and chemically couples the miR146a amino group to the CNP hydroxyl group.

Bleomycin injury animal model

C57BL/6 male mice, aged 8 to 10 weeks (strain No. 000642, Jackson Laboratory), were used for this study. All mice were maintained one week in standard housing to allow for acclimation to Denver ambient atmosphere (1600 m altitude) prior to use in the experiment. Animal study was approved by the Institutional Animal Care and Use Committee (IACUC, protocol #427) at the University of Colorado Denver–Anschutz Medial Campus (License #84-R-0059). Animal care was performed by trained veterinarians and technologists according to the NID Guide for the Care and Use of Laboratory Animals. Mice were injured with a single IT dose of 5 U/kg (2.94 mg/kg) bleomycin (Bleo) diluted to a concentration of 1.3 U/mL. Remaining mice were given an equivalent volume of phosphate buffered saline (PBS) for the uninjured control group (Control). Treatment of injured mice with CNP-miR146a was performed at three or seven days (Bleo + CNP-miR146a D3; Bleo + CNP-miR146a D7), as described below.

Intratracheal treatment with CNP-miR146a

CNP-miR146a toxicity studies have been previously described including a 3-(4,5-dimethylthiazol-2-yl)-2,5-diphenyl tetrazolium bromide (MTT) toxicity assay, comparative pathology, and systemic distribution analyses.[20] For this study, conjugated 100 ng of CNP-miR146a was diluted in 50 μL phosphate buffered solution (PBS) for intratracheal dosing. A subset of mice injured with bleomycin was treated with 100 ng/50 μL CNP-miR146a three days after injury or seven days after injury to evaluate for delayed treatment effect on reactive oxygen species (ROS) production, inflammation, fibrosis, and lung function. Previous study identified that the conjugate treatment performed better than individual component dosing (using CNP or miR146a mimetic alone), and therefore rescue treatment was only tested with CNP-miR146a to optimize animal use.[20] We utilized the control data initially published in our original prevention manuscript[20] in our comparison analysis with the delayed day three and seven treatment groups in an effort to ethically reduce animal numbers given the same endpoint in experiments. All measurements described below were taken from distinct samples.

ROS measurement with electron paramagnetic resonance (EPR) spectrometry

Whole lung tissue was harvested 14 days following injury ($n = 5$, 10, 12, 5 for Control, Bleo, Bleo + CNP-miR146a D3, and Bleo + CNP-miR146a D7, respectively) following pulmonary flushing with 5 mL of chilled PBS via right cardiac puncture. Tissue was homogenized using sucrose buffer (0.25 M sucrose, 10 mM Tris–

HCl, 1 mM EDTA, pH 7.4). Lung homogenate was mixed with Krebs-HEPES buffer (KHB), 100 μM DTPA (metal chelator), and 0.2 mM 1-hydroxy-3-methoxycarbonyl-2, 2, 5, 5-tetramethylpyrrolidine (CMH). CMH is a superoxide selective spin probe that reacts with superoxide to form the more stable CM• radical. CM• can then be detected by EPR and its concentration reflects ROS production. Samples were incubated for 60 min at 37 °C prior to loading 150 μL into rubber-top sealed PTFE tubing.[33] EPR acquisition was performed using the Bruker EMX nano- X-band spectrometer and CM• concentration was detected in the Bruker liquid nitrogen Finger Dewar at 77 K. CMH in KHB without the lung homogenate was used as a blank sample to determine the background signal, which was subtracted from the CM• signal. Double integration followed by Spin count using the Bruker software was used to measure CM• nitroxide radical concentration for each sample. The acquisition parameters used were: microwave frequency = 9.65 GHz; center field = 3438 G; modulation amplitude = 4.0 G; sweep width = 150 G; microwave power = 0.316 mW; total number of scans = 10; sweep time = 60 s; and time constant = 1.28 ms, as described previously.[20]

Inflammatory and fibrotic gene signaling measurement

Whole lung tissue was collected at 7 and 14 days following injury for real-time quantitative polymerase chain reaction (RT-qPCR) analysis of pro-inflammatory and pro-fibrotic gene expression. Three groups were evaluated at the seven-day timepoint (n = 6, 6, 7 for the Control, Bleo, and Bleo + CNP-miR146a D3 groups, respectively), while all four groups were evaluated at the fourteen-day timepoint (n = 6, 6, 6, 5 for Control, Bleo, Bleo + CNP-miR146a D3, and Bleo + CNP-miR146a D7, respectively). Collected lung tissue was flash frozen prior to homogenizing in Qiazol (Qiagen) per manufacturer instructions. RNA was isolated and converted to cDNA (Applied Biosystems RT kit). Amplification of cDNA was performed by reverse transcriptase amplification with the BioRad CFX-9600 thermal cycler. RT-qPCR was done for IL-6, IL-8, and TNFα for pro-inflammatory genes and collagen (Col) 1α2, Col3α1, and transforming growth factor (TGF)-β1 for pro-fibrotic genes, with glyyceraldehyde 3-phosphate dehydrogenase (GAPDH) used as the housekeeper gene for normalization. Each sample was analyzed in triplicate with the average of each triplicate used for normalization.

Immunohistochemistry for inflammatory cell infiltration and fibrosis

Histologic analysis of inflammatory cell infiltrate and collagen deposition was performed on lung tissue collected fourteen days after injury (n = 7, 7, 6, 7 for Control, Bleo, Bleo + CNP-miR146a D3, and Bleo + CNP-miR146a D7, respectively). Lungs were inflated with melted agarose solution and removed into 4% paraformaldehyde (PFA). The lung was immersion fixed in 4% PFA for 24 h at room temperature prior to dehydrating in 70% ethyl alcohol (EtOH). Dehydrated tissue was embedded into paraffin blocks and sectioned at four μm. Sectioned slides were stained with Mason's trichrome, which is a general collagen stain turning collagen fibers blue under bright field microscopy. Twenty high-powered fields (HPF) at 400× total magnification were randomly imaged for each sample. An automated counting algorithm on NIS Elements–Advanced Research imaging software was used by a blinded researcher to quantify the area of blue staining per HPF, which quantifies the area of collagen per HPF. The 20 random fields were averaged for each sample for comparison between groups.

Additional slides were deparaffinized for immunohistochemistry with CD45 staining. CD45 is a common leukocyte antigen that stains all leukocytes brown under bright field microscopy. The heat-induced epitope was acquired using the Biocare Medical Decloaker prior to slide staining with Leica's Bond Rx instrument. Slides were then treated with primary CD45 antibodies (1:50 solution, BD Biosciences) and developed with Vectastain Elite ABC kit (Vector laboratories). As above, 20 random 400× magnification HPFs were imaged and the number of CD45-positive cells per HPF was quantified. Average counts per HPF for each sample were used for analysis.

Lung mechanical function analysis following acute lung injury and rescue treatment

Mice underwent mechanical ventilation testing 14 days after injury to assess pulmonary function (n = 11, 8, 9, 9 for Control, Bleo, Bleo + CNP-miR146a D3, and Bleo + CNP-miR146a D7). For the ventilatory procedure, mice were anesthetized with acepromazine (2.5 mg/kg), ketamine (100 mg/kg), and xylazine (8 mg/kg) via intraperitoneal (IP) injection. A tracheostomy was performed using an 18-gauge cannula through which mice were ventilated using a computer-controlled small animal ventilator (SCIREQ flexiVent). Once on the ventilator, mice were given 0.8 mg/kg IP pancuronium bromide to suppress respiratory efforts that would invalidate the measurements of lung mechanics. All subjects underwent a 10-min stabilization period of baseline ventilation of 10 mL/kg tidal volume at 200 breaths per minute with positive end expiratory pressure (PEEP) = 3 cmH_20. Every two minutes the mice received a recruitment maneuver (RM) consisting of a 3-s ramp to 30 cmH_20 with a 3-s breath hold.

The lung mechanics assessment included an RM followed by a 16-s step-wise pressure-volume loop with a maximal pressure of 30 cmH_20, which was then used to calculate quasi-static compliance at 5 cmH_20 during expiration and the delivered volume, which we refer to as the inspiratory capacity. To measure pulmonary system impedance, an RM was performed and the baseline ventilation was applied at PEEP = 0 cmH_2O. Four 3-s multi-frequency forced oscillations (delivered volume 3 mL/kg, PEEP = 0 cmH_2O, 13 mutually prime frequencies from 1 to 20.5 Hz) were then applied at 10 s intervals. These impedance data were then used to determine pulmonary system elastance, tissue resistance, and airway resistance by fitting to the constant phase model.[34]

Statistical analyses

Quantitative variables were compared between groups using One-Way ANOVA for a significance value of $\alpha = 0.05$. Statistical analysis was performed with GraphPad Prism 9 (San Diego, CA).

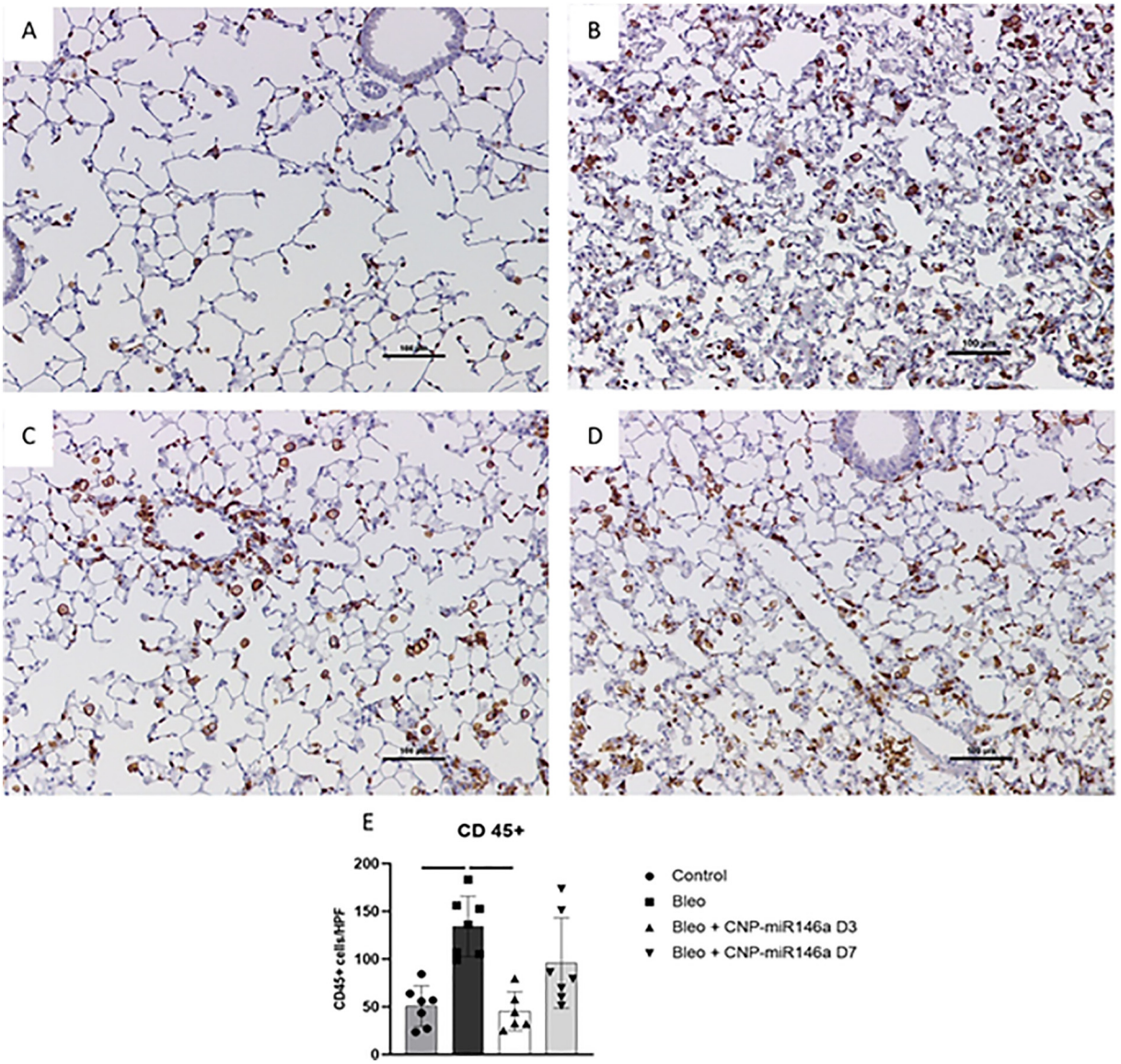

Figure 1. Decreased leukocyte infiltrate with CNP-miR146a within the lung.**(A-D)** 100× magnification slides stained for CD45 of lung tissue collected 14 days after injury. **(A)** Control, **(B)** Bleomycin, **(C)** Bleomycin + CNP-miR146a Day 3, **(D)** Bleomycin + CNP-miR146a day 7. **(E)** Quantitative analysis of CD45+ cells per high-powered field (HPF). CNP-miR146a given three days after bleomycin injury significantly lowered the number of CD45+ cells per HPF. Bars indicate statistical significance with $P < 0.05$. Mean and standard deviation values are shown; $n = 7, 7, 6, 7$ samples for Control, Bleo, Bleo + CNP-miR146a D3, and Bleo + CNP-miR146a D7, respectively.

Results

CNP-miR146a reduce inflammatory cell infiltrate

Immunohistochemical analysis of leukocyte infiltrate into pulmonary tissue was performed on samples collected 14 days after injury. Representative images at 100× magnification of CD45 + stained slides are shown in Figure 1, *A-D*. Qualitatively, control lungs had less alveolar collapse and debris than bleomycin-injured lungs. There were significantly more CD45+ cells per HPF in bleomycin-injured lungs than controls (P = 0.0004, 95% CI: [−131.5, −35.49]). The alveolar structure subjectively appeared more preserved in the bleomycin lungs treated with CNP-miR146a 3 days after injury (Figure 1, *C*). Quantitative analysis of CD45+ cells per HPF showed that treatment with CNP-miR146a on day 3 significantly lowered leukocyte infiltrate compared to untreated lungs (P = 0.0003, 95% CI: [38.94, 138.9]); however, treatment with CNP-miR146a seven days after injury did not significantly lower CD45+ cell counts (P = 0.1499).

Reduction in pro-inflammatory gene signaling with CNP-miR146a three and seven days after injury

Whole lung tissue was collected at 7 and 14 days following injury and processed for RT-qPCR to evaluate for relative gene expression of pro-inflammatory genes IL-6, IL-8, and TNFα. As depicted in Figure 2, *A-C*, bleomycin injury increased IL-6, IL-8, and TNFα gene expression 7 days after injury ($P < 0.0001$, 95%

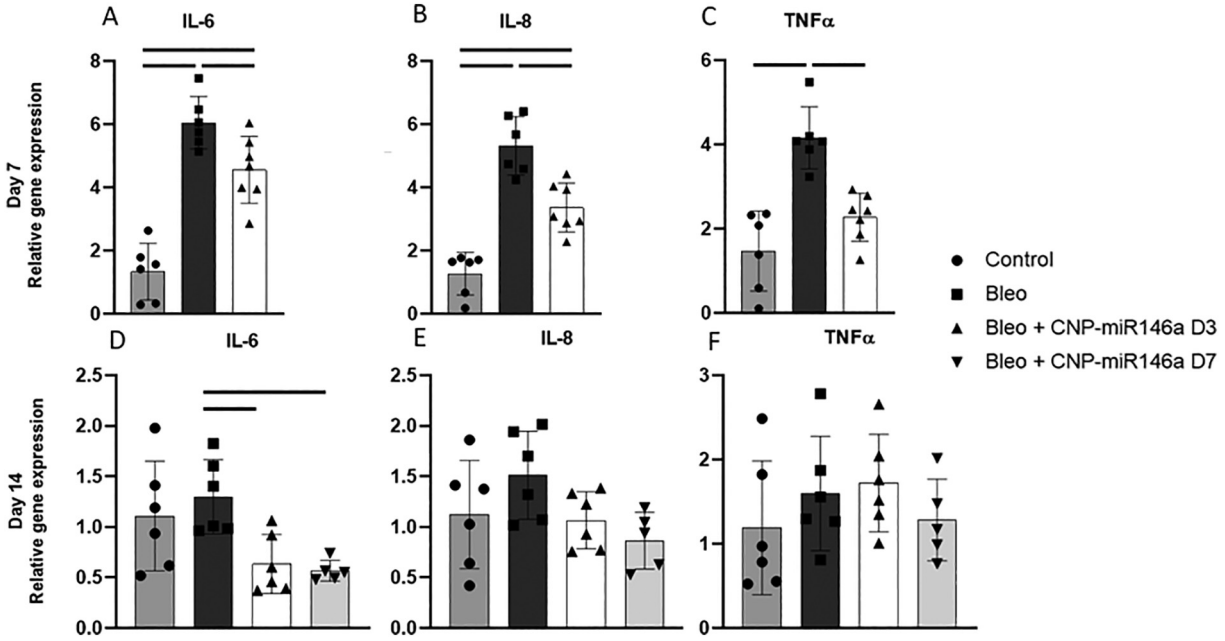

Figure 2. CNP-miR146a treatment three days after injury lowers pro-inflammatory gene signaling.Relative gene expression compared to GAPDH of IL-6 **(A, D)**, IL-8 **(B, E)**, and TNFα **(C, F)** both 7 **(A-C)** and 14 **(D-F)** days after injury. Bleomycin injury resulted in significantly higher IL-6, IL-8, and TNFα gene expression seven days after injury **(A-C)**, but gene expression was no different at two weeks **(D-F)**. CNP-miR146a, when given three days after injury, significantly lowered IL-6, IL-8, and TNFα gene expression compared to untreated, bleomycin-injured lungs. Bars indicate statistical significance with $P < 0.05$. Mean and standard deviation values are shown for $n = 6, 6, 7$ samples at day seven for the Control, Bleo, and Bleo + CNP-miR146a D3 groups, respectively, and for $n = 6, 6, 6, 5$ samples at day fourteen for Control, Bleo, Bleo + CNP-miR146a D3, and Bleo + CNP-miR146a D7, respectively.

CI: [−6.12, −3.31]; $P < 0.0001$, 95% CI: [−5.23, −2.87]; $P < 0.0001$, 95% CI: [−3.81, −1.59]). A single treatment with CNP-miR146a at day 3 following injury lowered TNFα gene expression to control levels at day 7 (Figure 2, *C*). IL-6, IL-8, and TNFα relative gene expressions were all lower 7 days after injury with CNP-miR146a treatment at day 3 when compared to bleomycin-injured lungs ($P = 0.0293$, 95% CI: [1.87, 5.57]; $P = 0.0012$, 95% CI: [0.81, 3.09]; $P = 0.0011$, 95% CI: [0.80, 2.97]).

Fourteen days following injury, IL-6, IL-8, and TNFα relative gene expression returned to control levels in untreated, bleomycin-injured lungs (Figure 2, *D-F*). Treatment with CNP-miR146a three and seven days after injury resulted in decreased IL-6 gene expression compared to bleomycin-injured lungs at day 14 ($P = 0.0278$, 95% CI: [0.06, 1.27]; $P = 0.0199$, 95% CI: [0.10, 1.36]). IL-8 and TNFα gene expression was not significantly different between any groups at day 14.

CNP-miR146a lowers ROS concentration in the lung

Lung tissue harvested 14 days following bleomycin injury was measured with electron paramagnetic resonance (EPR) spectrometry for CM• concentration, which reflects ROS concentration. Lungs injured with bleomycin had significantly higher CM• concentrations compared to controls ($P = 0.0241$, 95% CI: [−81.68, −4.54]). Rescue treatment with CNP-miR146a at both 3 days and 7 days lowered ROS levels compared to bleomycin-injured lungs ($P = 0.0049$, 95% CI: [10.65, 70.96]; $P = 0.0414$, 95% CI: [1.21, 78.35], returning CM• concentrations to control levels as depicted in Figure 3.

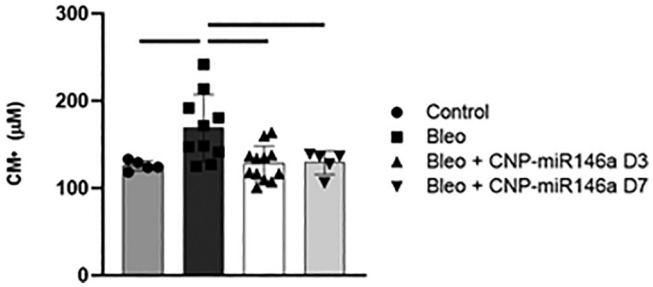

Figure 3. Bleomycin increases ROS as measured by EPR, rescued by CNP-miR146a.Fourteen days after injury, CM• concentration is significantly lower in control, day 3-treated, and day 7-treated lungs compared to untreated, bleomycin-injured lungs. Bars indicate statistical significance with $P < 0.05$. Mean and standard deviation values are shown for $n = 5, 10, 12, 5$ samples for Control, Bleo, Bleo + CNP-miR146a D3, and Bleo + CNP-miR146a D7, respectively.

Rescue from pro-fibrotic gene signaling with CNP-miR146a

Quantitative PCR analyzing the relative gene expression of Col1α2, Col3α1, and TGFβ-1 was performed on days seven and fourteen after initial injury. Pro-fibrotic gene expression in lungs treated with CNP-miR146a three days after injury returned to control levels, with significantly lower expression levels of Col1α2, Col3α1, and TGFβ-1 compared to untreated, bleomycin-injured lungs on day seven (Figure 4, *A-C*, $P = 0.0161$, 95% CI: [0.10, 0.94]; $P = 0.0023$, 95% CI: [0.30, 1.21]; $P = 0.0254$, 95% CI: [0.06, 0.90]). Bleomycin injured lungs had

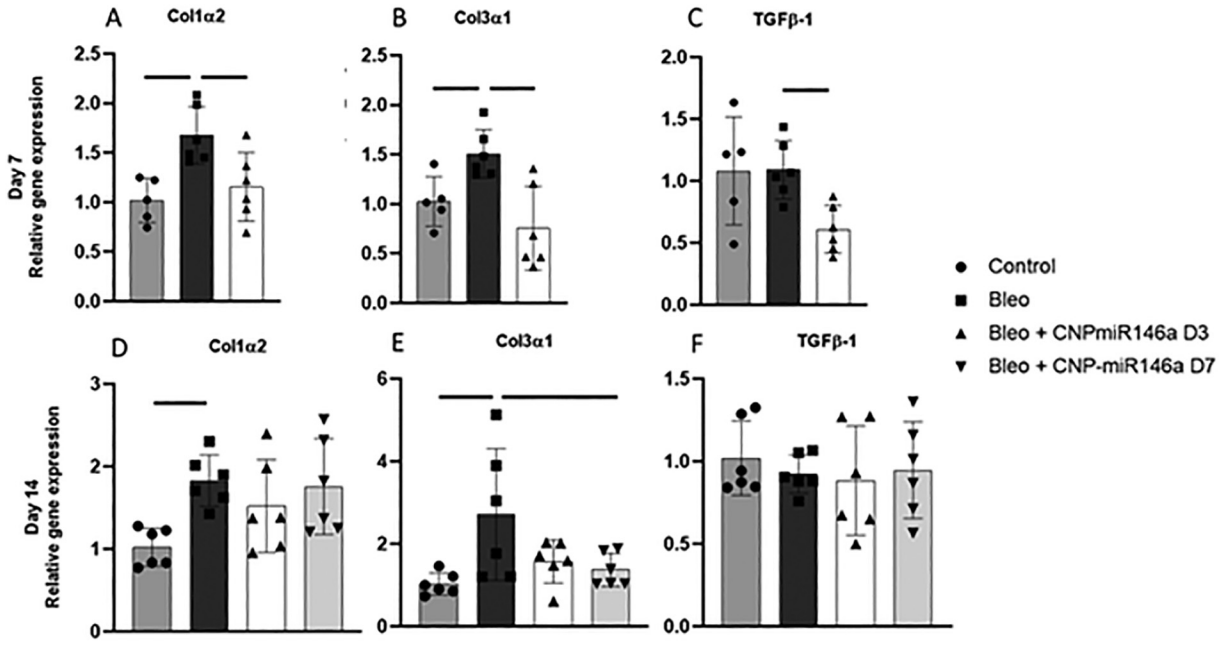

Figure 4. Pro-fibrotic gene signaling is attenuated with CNP-miR146a.Relative gene expression compared to GAPDH of Col1α2 **(A, D)**, Col3α1 **(B, E)**, and TGFβ-1 **(C, F)** both 7 **(A-C)** and 14 **(D-F)** days after injury. Bleomycin injury increased Col1α2 and Col3α1 gene expression seven and fourteen days after injury. Treatment with CNP-miR146a 3 days after injury significantly lowered Col1α2 and Col3α1 gene expression at seven days, also lowering TGFβ-1 at this timepoint. Treatment with CNP-miR146a seven days after injury lowered Col3α1 gene expression compared to untreated, bleomycin-injured lungs 14 days after injury. Bars indicate statistical significance with $P < 0.05$. Mean and standard deviation values are shown for $n = 6, 6, 7$ samples at day seven for the Control, Bleo, and Bleo + CNP-miR146a D3 groups, respectively, and for $n = 6, 6, 6, 5$ samples at day fourteen for Control, Bleo, Bleo + CNP-miR146a D3, and Bleo + CNP-miR146a D7, respectively.

higher Col1α2 and Col3α1 expression levels than controls at day seven ($P = 0048$, 95% CI: [0.22, 1.10]; $P = 0.0475$, 95% CI: [0.01, 0.96]).

Fourteen days after injury Col1α2 and Col3α1 expression remained significantly higher in bleomycin-injured lungs compared to uninjured lungs (Figure 4, *D-E*, $P = 0.0145$, 95% CI: [0.15, 1.42]; $P = 0.0091$, 95% CI: [0.40, 2.97]). Expression levels of Col1α2, Col3α1, and TGFβ-1 after rescue treatment with CNP-miR146a three days after injury were not significantly different from controls or bleomycin mice at day fourteen. Mice treated seven days after injury had significantly lower Col3α1 gene expression than untreated mice ($P = 0.0400$, 95% CI: [0.05, 2.62]).

Histologic improvement in collagen deposition with CNP-miR146a three days after injury

Quantitative analysis of trichrome stained slides was performed for samples collected 14 days after injury as an assessment of collagen levels in the lung. Representative images at 100× total magnification (10× objective lens) of trichrome stained samples are shown in Figure 5, *A-D*. Bleomycin-injured lungs had significantly greater area per HPF that was positively stained for collagen (blue) compared to control lungs ($P = 0.0179$, 95% CI: [−131.5, −35.49]). Treatment with CNP-miR146a 3-days following injury, but not 7 days after injury, lowered the quantitative level of collagen per HPF compared to untreated specimens ($P = 0.0244$, 95% CI: [38.94, 138.9], $P = 0.1499$, 95% CI: [−9.64, 86.41]).

CNP-miR146a rescues pulmonary function

Pulmonary mechanics were measured 14 days after injury during invasive mechanical ventilation. Multi-frequency forced oscillation measurements at PEEP = 0 cmH_2O show that bleomycin-injured mice had significantly higher pulmonary system elastance and tissue resistance than control mice (Figure 6, *A*, *D*; $P = 0.0002$, 95% CI: [−33.47, −9.43]; $P < 0.0001$, 95% CI: [−5.04, −1.05]). Treatment with CNP-miR146a three days after injury rescued pulmonary elastance to control levels, with significantly lower elastance than untreated mice ($P = 0.0195$, 95% CI: [1.82, 26.42]). Treatment at seven days did not improve elastance or tissue resistance compared to untreated mice. In all cases, airway resistance was not different between groups (data not shown). Similarly, bleomycin injury resulted in lower quasi-static compliance and inspiratory capacity compared to control mice (Figure 6, *B*, *C*; $P < 0.0001$, 95% CI: [0.02, 0.04]; $P < 0.0001$, 95% CI: [0.14, 0.33]). CNP-miR146a administration three days after bleomycin injury significantly improved compliance and inspiratory capacity compared to untreated mice ($P = 0.0482$, 95% CI: [−0.02, 0]; $P = 0.0230$, 95% CI: [−0.21, −0.01]).

Discussion

In this study, we have demonstrated that a single dose of CNP-miR146a three days after the onset of ALI due to bleomycin is able to improve pulmonary mechanics. Previously shown to prevent inflammation, oxidative stress, and fibrosis with co-treatment at the time of injury, this study highlights that

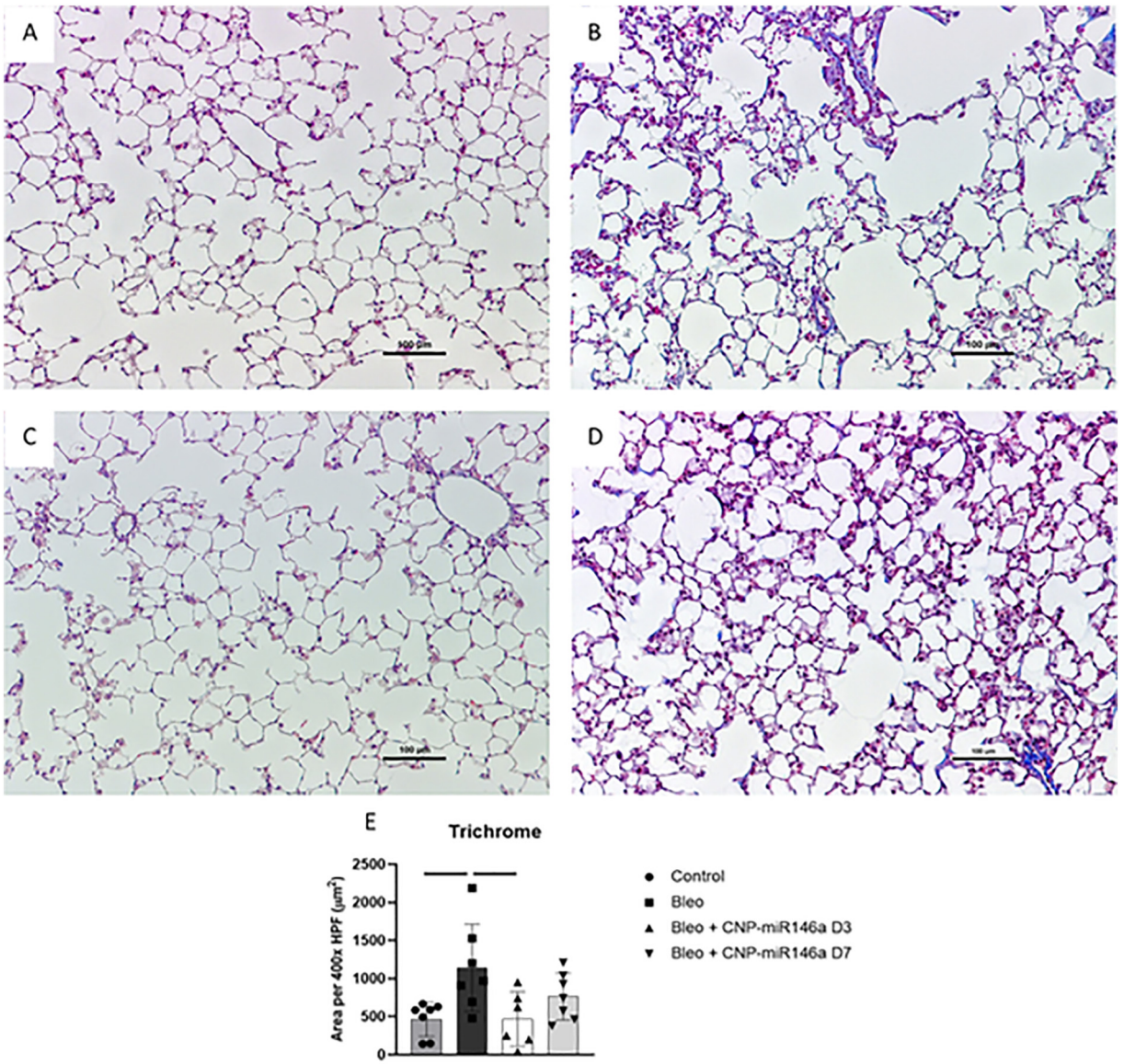

Figure 5. CNP-miR146a lowers histologic quantification of lung collagen.**(A-D)** 100× magnification slides stained for CD45 of lung tissue collected 14 days after injury. **(A)** Control, **(B)** Bleomycin, **(C)** Bleomycin + CNP-miR146a Day 3, **(D)** Bleomycin + CNP-miR146a day 7. **(E)** Quantitative analysis of area of trichrome staining per high-powered field (HPF). CNP-miR146a treatment three days after injury significantly lowered collagen area per HPF compared to the Bleomycin injury group. Bars indicate statistical significance with $P < 0.05$. Mean and standard deviation values are shown for $n = 7, 7, 6, 7$ samples for Control, Bleo, Bleo + CNP-miR146a D3, and Bleo + CNP-miR146a D7, respectively.

IT delivery of CNP-miR146a in a delayed fashion after ALI onset is able to still inhibit the inflammatory and fibrotic processes, ultimately improving lung mechanics.

CNP-miR146a attenuated the increase seen in bleomycin-induced pro-inflammatory gene expression when delivered as a rescue therapy, as depicted in Figure 2. Human ARDS is associated with increased circulating levels of TNFα, IL-6, and IL-8, important mediators and markers of inflammation.[35,36] Patients with novel coronavirus-associated ARDS have higher IL-6 and TNFα levels and have increased risk of requiring mechanical ventilation and mortality.[11,12] MiR146a inhibits IRAK1 and TRAF6, upstream promotors of NFκB, which in turn inhibit IL-6, IL-8, and TNFα.[15–18] CNP-miR146a increases miR146a levels in the lung following IT delivery,[20] and this activation of intrinsic anti-inflammatory pathways may protect the lung from ongoing tissue damage and therefore improve function.

A possible pathway by which CNP-miR146a lowers inflammation is through reduction in pro-inflammatory signaling, as described above, but it may additionally contribute to a decrease in leukocyte recruitment to the site of injury. Leukocyte response to acute lung injury is complex, but involves rapid recruitment of circulating neutrophils and activation of alveolar macrophages.[37,38] These cell lines increase signaling cytokines and chemokines such as TNFα, TGFβ-1, and monocyte chemoattractant protein-1 (MCP-1) to recruit additional

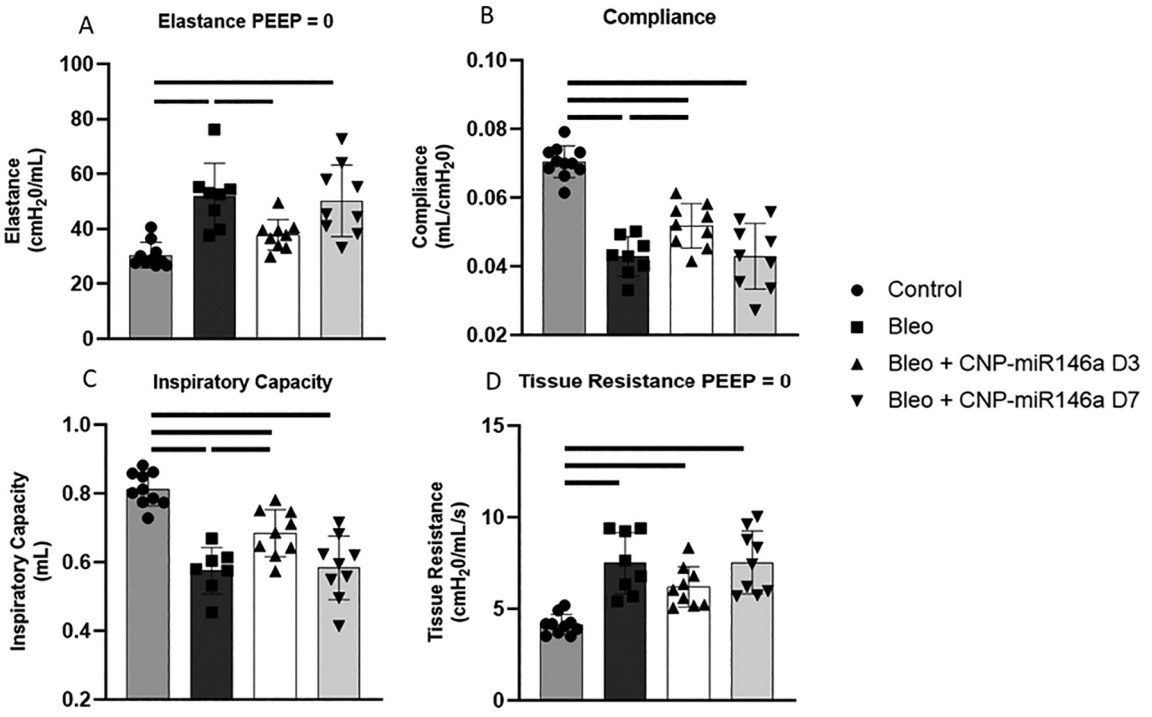

Figure 6. Treatment with CNP-miR146a three days after injury rescues lung function.**(A)** Pulmonary elastance and **(D)** tissue resistance are increased, and **(B)** quasi-static compliance and **(C)** inspiratory capacity are lowered, with bleomycin injury. CNP-miR146a treatment three days after injury significantly improves elastance, quasi-static compliance, and inspiratory capacity to control levels. Bars indicate statistical significance with $P < 0.05$. Mean and standard deviation are shown for $n = 11, 8, 9, 9$ samples for Control, Bleo, Bleo + CNP-miR146a D3, and Bleo + CNP-miR146a D7, respectively.

monocytes to the area. CD45 is a common leukocyte marker, so it reflects total leukocyte infiltration rather than specific cell lines, and we saw significantly lower CD45 cells in the lung with CNP-miR146a treatment 3 days after injury. Future investigation of whether the reduction in pro-inflammatory gene signaling and ROS could be secondary to a decrease in overall leukocyte infiltration, a change in leukocyte plasticity, or a combination of these conditions will help better elucidate the mechanisms of ARDS pathophysiology and the potential cell-level implications of CNP-miR146a as a therapy. Cellular level studies looking at the specific cell lines recruited to the site of injury, as well as the effect of CNP-miR146a on alveolar and interstitial macrophage recruitment and polarization, will better identify the direct mechanism by which CNP-miR146a decrease inflammatory signaling.

CNP are divalent metal oxides with ROS scavenging properties, offering a potential benefit in reducing oxidative stress in ALI and ARDS, which is characterized by excess ROS.[23,24,39] CNP and CNP-miR146a have been more fully characterized in our previous work with diabetic wounds.[40] Briefly, CNP and CNP-miR146a have a size of 20 nm and 190 nm, respectively, and conjugation of CNP to miR-146a significantly alters surface zeta charge while maintaining redox potential. High doses of CNP, up to 2000 μg/mL, which is over 1000 times the dose tested in this experiment, have been shown to have no toxicity to cell lines after 24 h of high-dose exposure.[41,42] We have previously shown similar data showing no cellular toxicity with CNP or CNP-miR146a. Additionally, IT CNP-miR146a do not increase plasma or lung CNP concentration 72 to 168 h after exposure, suggesting these lower doses may be adequately cleared with lower potential for toxicity.[20] The conjugation of CNP to miR146a could synergistically lower ROS, as miR146a modulates ROS production through the inhibition of cytokine signaling. We have previously shown that both CNP and miR146a alone can prevent ROS elevations in a bleomycin lung injury model.[20,43] Increased production of ROS promotes collagen formation and fibroblast proliferation, and ROS activates TGFβ-1, further increasing the pro-fibrotic response.[44–46]

Delayed treatment with CNP-miR146a attenuated pro-fibrotic gene expression and lowered collagen levels in the lung, as seen in Figures 4 and 5. The long-term effects of ARDS in survivors often manifest as fibrotic changes in the lung.[5,6] Survivors of ARDS have an exercise capacity at 66% of predicted and a mere 49% of patients return to work in the first year following hospitalization.[47] Extracellular matrix (ECM) remodeling in ARDS is multifactorial; however, pathways known to induce ARDS-associated fibrosis include TGFβ signaling and alterations in collagen types I and III.[13] The lung parenchyma is largely composed of type I and type III collagen fibers, and fibrotic remodeling is characterized by increased Col1α2 gene expression and higher collagen I-to-III protein ratios.[48] Trichrome is a general collagen marker, and therefore, we are unable to differentiate whether the histologic changes seen two weeks following injury with bleomycin are due to increases in collagen 1 or collagen 3 protein; however, CNP-miR146a lowers Col1α2, Col3α1, and TGFβ-1 signaling, potentially through alterations in ROS activation of ECM

pathways. By lowering pro-fibrotic gene signaling and overall collagen levels, CNP-miR146a could have the potential to improve long-term clinical effects while also improving lung function.

Ultimately, the goal of treatment is preservation of pulmonary function, and CNP-miR146a improved lung function at two weeks when given three days after injury, as depicted in Figure 6. Human ARDS is characterized by significant reductions in pulmonary system compliance due to inflammatory cell induction of alveolar collapse and pulmonary edema, and lower available lung volume is reflected in higher elastance.[49,50] While delaying treatment to seven days did not improve mechanical lung function following ALI, there were improvements in ROS and pro-inflammatory signaling. It is possible that our end-point of 14 days did not provide enough time for any functional improvement to be identified secondary to CNP-miR146a instillation seven days after injury. Future study to evaluate later timepoints and if higher doses of CNP-miR146a at later timepoints may improve lung function will be important for determining the optimal treatment window for ALI with CNP-miR146a. CNP-miR146a could therefore have implications clinically in reducing the need for mechanical ventilation or duration of mechanical ventilation through rescuing of pulmonary mechanics even after inflammatory and oxidative stress pathways have been activated.

ALI and ARDS pathophysiology in humans is multi-factorial in etiology and pathogenesis, so a wide range of pre-clinical models, such as lipopolysaccharide (LPS)-induced lung injury, are used. We chose to use the bleomycin-induced lung injury as it is a well-established lung injury model secondary to its long-term fibrotic effects and well accepted mechanism of injury, and it is a continuation of our previous work with CNP-miR146a co-treatment at the time of injury.[20] Future study utilizing different models, such as LPS-induced lung injury and ventilator-induced lung injury, will help to generalize the utility of CNP-miR146a as a rescue treatment for ALI. The dose chosen for this study was based on work performed in both diabetic wounds and bleomycin-induced lung injury.[20,51] In our work with diabetic wounds, higher doses of CNP-miR146a delayed wound healing, which we hypothesized was secondary to the need for some inflammation to promote healing. We therefore wished to look at this established dose in treating ALI in a delayed fashion, and future evaluation of a dose–response will be undertaken specifically looking at the effect on pulmonary function, toxicity, and cellular uptake.

CNP and miR146a have been shown to have potential applications in treating acute lung injury.[14,18,19,27,52] We have previously shown that IT delivery of CNP-miR146a has low toxicity with local delivery and no systemic uptake, and that the conjugate treatment of CNP-miR146a is able to prevent ALI better than the individual component doses.[20] While there have been advancements in understanding the pathogenesis of ARDS, mortality remains high and therapeutic innovation is of critical importance. This study is the first to look at the potential of CNP-miR146a in treating ALI/ARDS using a delayed treatment strategy, which has greater clinical implications than a preventative therapy. In this study, we have shown that treatment with CNP-miR146a three days after injury improves pulmonary function by lowering pro-inflammatory gene expression and oxidative stress, reducing leukocyte infiltration, and decreasing pro-fibrotic gene expression and collagen levels in the lung.

Credit Author Statement

Stephen M. Niemiec: Conceptualization, data curation, formal analysis, investigation, methodology, project administration, visualization, roles/writing – original draft, writing – review & editing.

Sarah A. Hilton: Conceptualization, data curation, formal analysis, investigation, methodology, project administration, visualization, roles/writing – original draft, writing – review & editing.

Alison Wallbank: Data curation, investigation, methodology, project administration, writing – review & editing.

Amanda E. Louiselle: Data curation, investigation, methodology, project administration, writing – review & editing.

Hanan Elajaili: Data curation, investigation, methodology, project administration, writing – review & editing.

Junyi Hu: Data curation, investigation, methodology, project administration, resources, writing – review & editing.

Sushant Singh: Data curation, investigation, methodology, project administration, resources, writing – review & editing.

Sudipta Seal: Conceptualization, funding acquisition, project administration, supervision, validation, writing – review & editing.

Eva Nozik-Grayck: Conceptualization, funding acquisition, project administration, supervision, validation, writing – review & editing.

Bradford Smith: Conceptualization, funding acquisition, project administration, supervision, validation, writing – review & editing.

Carlos Zgheib: Conceptualization, funding acquisition, project administration, supervision, validation, writing – review & editing.

Kenneth W. Liechty: Conceptualization, funding acquisition, project administration, supervision, validation, writing – review & editing.

Acknowledgments

The authors would like to thank the University of Colorado Denver Histology Shared Resource Center for their contribution to this work. This work was supported by a Gates Center Grubstake Award for the work presented in this publication.

References

1. Matthay MA, Zemans RL, Zimmerman GA, Arabi YM, Beitler JR, Mercat A, et al. Acute respiratory distress syndrome. *Nat Rev Dis Primers* 2019;**5**(1):18.
2. Pierrakos C, Karanikolas M, Scolletta S, Karamouzos V, Velissaris D. Acute respiratory distress syndrome: pathophysiology and therapeutic options. *J Clin Med Res* 2012;**4**(1):7-16.
3. Hasan Z. A review of acute respiratory distress syndrome management and treatment. *Am J Ther* 2021;**28**(2):e189-95.
4. Bellani G, Laffey JG, Pham T, Fan E, Brochard L, Esteban A, et al. Epidemiology, patterns of care, and mortality for patients with acute respiratory distress syndrome in intensive care units in 50 countries. *JAMA* 2016;**315**(8):788-800.

5. DiSilvio B, Young M, Gordon A, Malik K, Singh A, Cheema T. Complications and outcomes of acute respiratory distress syndrome. *Crit Care Nurs Q* 2019;**42**(4):349-61.
6. Desai SR, Wells AU, Rubens MB, Evans TW, Hansell DM. Acute respiratory distress syndrome: CT abnormalities at long-term follow-up. *Radiology* 1999;**210**(1):29-35.
7. Griffiths MJD, McAuley DF, Perkins GD, Barrett N, Blackwood B, Boyle A, et al. Guidelines on the management of acute respiratory distress syndrome. *BMJ Open Respir Res* 2019;**6**(1)e000420.
8. Grulke E, Reed K, Beck M, Huang X, Cormack A, Seal S. Nanoceria: factors affecting its pro- and anti-oxidant properties. *Environ Sci-Nano* 2014;**1**(5):429-44.
9. Schwartz MD, Moore EE, Moore FA, Shenkar R, Moine P, Haenel JB, et al. Nuclear factor-kappa B is activated in alveolar macrophages from patients with acute respiratory distress syndrome. *Crit Care Med* 1996;**24**(8):1285-92.
10. Selvaraj V, Nepal N, Rogers S, Manne ND, Arvapalli R, Rice KM, et al. Inhibition of MAP kinase/NF-kB mediated signaling and attenuation of lipopolysaccharide induced severe sepsis by cerium oxide nanoparticles. *Biomaterials* 2015;**59**:160-71.
11. Herold T, Jurinovic V, Arnreich C, Lipworth BJ, Hellmuth JC, von Bergwelt-Baildon M, et al. Elevated levels of IL-6 and CRP predict the need for mechanical ventilation in COVID-19. *J Allergy Clin Immunol* 2020;**146**(1):128-36 e4.
12. Mortaz E, Tabarsi P, Jamaati H, Dalil Roofchayee N, Dezfuli NK, Hashemian SM, et al. Increased serum levels of soluble TNF-alpha receptor is associated with ICU mortality in COVID-19 patients. *Front Immunol* 2021;**12**592727.
13. Vishnupriya M, Naveenkumar M, Manjima K, Sooryasree NV, Saranya T, Ramya S, et al. Post-COVID pulmonary fibrosis: therapeutic efficacy using with mesenchymal stem cells - how the lung heals. *Eur Rev Med Pharmacol Sci* 2021;**25**(6):2748-51.
14. Liu J, Sala MA, Kim J. Dampening the fire: a negative feedback loop in acute respiratory distress syndrome. *Am J Respir Cell Mol Biol* 2021;**64**(2):158-60.
15. An R, Feng J, Xi C, Xu J, Sun L. miR-146a attenuates sepsis-induced myocardial dysfunction by suppressing IRAK1 and TRAF6 via targeting ErbB4 expression. *Oxidative Med Cell Longev* 2018;**2018**:7163057.
16. Blackwell TS, Christman JW. The role of nuclear factor-kappa B in cytokine gene regulation. *Am J Respir Cell Mol Biol* 1997;**17**(1):3-9.
17. Chen J, Hu C, Pan P. Extracellular vesicle microRNA transfer in lung diseases. *Front Physiol* 2017;**8**:1028.
18. Zeng Z, Gong H, Li Y, Jie K, Ding C, Shao Q, et al. Upregulation of miR-146a contributes to the suppression of inflammatory responses in LPS-induced acute lung injury. *Exp Lung Res* 2013;**39**(7):275-82.
19. Bobba CM, Fei Q, Shukla V, Lee H, Patel P, Putman RK, et al. Nanoparticle delivery of microRNA-146a regulates mechanotransduction in lung macrophages and mitigates injury during mechanical ventilation. *Nat Commun* 2021;**12**(1):289.
20. Niemiec SM, Hilton SA, Wallbank A, Azeltine M, Louiselle AE, Elajaili H, et al. Cerium oxide nanoparticle delivery of microRNA-146a for local treatment of acute lung injury. *Nanomedicine* 2021;**34**102388.
21. Chen J, Patil S, Seal S, McGinnis JF. Rare earth nanoparticles prevent retinal degeneration induced by intracellular peroxides. *Nat Nanotechnol* 2006;**1**(2):142-50.
22. Dowding JM, Song W, Bossy K, Karakoti A, Kumar A, Kim A, et al. Cerium oxide nanoparticles protect against Abeta-induced mitochondrial fragmentation and neuronal cell death. *Cell Death Differ* 2014;**21**(10):1622-32.
23. Heckert EG, Karakoti AS, Seal S, Self WT. The role of cerium redox state in the SOD mimetic activity of nanoceria. *Biomaterials* 2008;**29**(18):2705-9.
24. Korsvik C, Patil S, Seal S, Self WT. Superoxide dismutase mimetic properties exhibited by vacancy engineered ceria nanoparticles. *Chem Commun (Camb)* 2007;**10**:1056-8.
25. Pirmohamed T, Dowding JM, Singh S, Wasserman B, Heckert E, Karakoti AS, et al. Nanoceria exhibit redox state-dependent catalase mimetic activity. *Chem Commun (Camb)* 2010;**46**(16):2736-8.
26. Sack M, Alili L, Karaman E, Das S, Gupta A, Seal S, et al. Combination of conventional chemotherapeutics with redox-active cerium oxide nanoparticles—a novel aspect in cancer therapy. *Mol Cancer Ther* 2014;**13**(7):1740-9.
27. Allawadhi P, Khurana A, Allwadhi S, Joshi K, Packirisamy G, Bharani KK. Nanoceria as a possible agent for the management of COVID-19. *Nano Today* 2020;**35**100982.
28. Kumari P, Saifi MA, Khurana A, Godugu C. Cardioprotective effects of nanoceria in a murine model of cardiac remodeling. *J Trace Elem Med Biol* 2018;**50**:198-208.
29. Fahy RJ, Lichtenberger F, McKeegan CB, Nuovo GJ, Marsh CB, Wewers MD. The acute respiratory distress syndrome: a role for transforming growth factor-beta 1. *Am J Respir Cell Mol Biol* 2003;**28**(4):499-503.
30. Garbuzenko OB, Saad M, Betigeri S, Zhang M, Vetcher AA, Soldatenkov VA, et al. Intratracheal versus intravenous liposomal delivery of siRNA, antisense oligonucleotides and anticancer drug. *Pharm Res* 2009;**26**(2):382-94.
31. Karakoti AS, Monteiro-Riviere NA, Aggarwal R, Davis JP, Narayan RJ, Self WT, et al. Nanoceria as antioxidant: synthesis and biomedical applications. *JOM (1989)* 2008;**60**(3):33-7.
32. Patil S, Kuiry SC, Seal S, Vanfleet R. Synthesis of nanocrystalline ceria particles for high temperature oxidation resistant coating. *J Nanopart Res* 2002;**4**(5):433-8.
33. Elajaili HB, Hernandez-Lagunas L, Ranguelova K, Dikalov S, Nozik-Grayck E. Use of electron paramagnetic resonance in biological samples at ambient temperature and 77 K. *J Vis Exp* 2019;**143**.
34. Hantos Z, Daroczy B, Suki B, Nagy S, Fredberg JJ. Input impedance and peripheral inhomogeneity of dog lungs. *J Appl Physiol (1985)* 1992;**72**(1):168-78.
35. Butt Y, Kurdowska A, Allen TC. Acute lung injury: a clinical and molecular review. *Arch Pathol Lab Med* 2016;**140**(4):345-50.
36. Spadaro S, Park M, Turrini C, Tunstall T, Thwaites R, Mauri T, et al. Biomarkers for acute respiratory distress syndrome and prospects for personalised medicine. *J Inflamm (Lond)* 2019;**16**:1.
37. Cheng P, Li S, Chen H. Macrophages in lung injury, repair, and fibrosis. *Cells* 2021;**10**(2).
38. Lin WC, Fessler MB. Regulatory mechanisms of neutrophil migration from the circulation to the airspace. *Cell Mol Life Sci* 2021;**78**(9):4095-124.
39. Kellner M, Noonepalle S, Lu Q, Srivastava A, Zemskov E, Black SM. ROS signaling in the pathogenesis of acute lung injury (ALI) and acute respiratory distress syndrome (ARDS). *Adv Exp Med Biol* 2017;**967**:105-37.
40. Niemiec SM, Louiselle AE, Hilton SA, Dewberry LC, Zhang L, Azeltine M, et al. Nanosilk increases the strength of diabetic skin and delivers CNP-miR146a to improve wound healing. *Front Immunol* 2020;**11**590285.
41. De Marzi L, Monaco A, De Lapuente J, Ramos D, Borras M, Di Gioacchino M, et al. Cytotoxicity and genotoxicity of ceria nanoparticles on different cell lines in vitro. *Int J Mol Sci* 2013;**14**(2):3065-77.
42. Singh S, Ly A, Das S, Sakthivel TS, Barkam S, Seal S. Cerium oxide nanoparticles at the nano-bio interface: size-dependent cellular uptake. *Artif Cells Nanomed Biotechnol* 2018;**46**(sup3):S956-63.
43. He L, Wang Z, Zhou R, Xiong W, Yang Y, Song N, et al. Dexmedetomidine exerts cardioprotective effect through miR-146a-3p targeting IRAK1 and TRAF6 via inhibition of the NF-kappaB pathway. *Biomed Pharmacother* 2021;**133**110993.
44. Cheresh P, Kim SJ, Tulasiram S, Kamp DW. Oxidative stress and pulmonary fibrosis. *Biochim Biophys Acta* 2013;**1832**(7):1028-40.
45. Koli K, Myllarniemi M, Keski-Oja J, Kinnula VL. Transforming growth factor-beta activation in the lung: focus on fibrosis and reactive oxygen species. *Antioxid Redox Signal* 2008;**10**(2):333-42.
46. Sambo P, Baroni SS, Luchetti M, Paroncini P, Dusi S, Orlandini G, et al. Oxidative stress in scleroderma: maintenance of scleroderma fibroblast phenotype by the constitutive up-regulation of reactive oxygen species

generation through the NADPH oxidase complex pathway. *Arthritis Rheum* 2001;**44**(11):2653-64.

47. Cheung AM, Tansey CM, Tomlinson G, Diaz-Granados N, Matte A, Barr A, et al. Two-year outcomes, health care use, and costs of survivors of acute respiratory distress syndrome. *Am J Respir Crit Care Med* 2006; **174**(5):538-44.
48. Ito JT, Lourenco JD, Righetti RF, Tiberio I, Prado CM, Lopes F. Extracellular matrix component remodeling in respiratory diseases: what has been found in clinical and experimental studies? *Cell* 2019;**8**(4).
49. Goligher EC, Costa ELV, Yarnell CJ, Brochard LJ, Stewart TE, Tomlinson G, et al. Effect of lowering tidal volume on mortality in ARDS varies with respiratory system Elastance. *Am J Respir Crit Care Med* 2021;**203**(11):1378-85.
50. Russotto V, Bellani G, Foti G. Respiratory mechanics in patients with acute respiratory distress syndrome. *Ann Transl Med* 2018;**6**(19):382.
51. Zgheib C, Hilton SA, Dewberry LC, Hodges MM, Ghatak S, Xu J, et al. Use of cerium oxide nanoparticles conjugated with MicroRNA-146a to correct the diabetic wound healing impairment. *J Am Coll Surg* 2019; **228**(1):107-15.
52. Ghadiali SN, Bobba C, Ballinger MN, Englert JA. Nanoparticle-based delivery of MicroRNA-146a mitigates ventilator induced lung injury and inflammation. *Am J Resp Crit Care* 2019;**199**.